MITIGATION OF BEAMFORMING INTERFERENCE FROM CLOSED WIND TUNNELS USING CLEAN-SC

Alexander Quayle*, Will Graham, Ann Dowling, Holger Babinsky, Yu Liu
Cambridge University Engineering Dept, Cambridge, England.

ABSTRACT

The Markham aerodynamic wind tunnel at Cambridge has been used for a series of aeroacoustic investigations into noise from landing gears and wing slats. This tunnel uses a pair of nested arrays to determine source strength across a range of frequencies. In the course of experiments it has been found that measurements from the smaller, high frequency array can under-estimate source strength at frequencies where the two arrays are expected to overlap. The effect on the spectrum was to mask lower level sources. As a result, the noise reduction available from a particular configuration could appear significantly larger than is actually the case.

In this paper we present a discussion of measurements from the tunnel and mechanisms for interference from wind tunnel sources. We confirm the existence of the effect using sources in an anechoic chamber. We also present a method for mitigating interference using the 'CLEAN-SC' algorithm with appropriately reshaped scanning grids for beamforming.

Results show that more consistent measurements are obtained from the two acoustic arrays, providing some validation of the method. This analysis has the potential to be significant in a variety of closed wind tunnel testing.

*arq20@cam.ac.uk

1 INTRODUCTION

Closed circuit wind tunnels are now regularly used for acoustic array measurements[1-4]. The closed circuit tunnel is often more readily available and may even allow simultaneous aerodynamic and acoustic testing. However, the measurement of noise sources in aerodynamic tunnels requires cautious interpretation of the results. Noise levels measured at the microphones may be 20dB or more above the signal of interest.

The capture of model source power from the high level background and boundary layer noise in a closed wind tunnel relies on removal of auto-power terms from the cross power matrix[5]. This helps to eliminate sound generated by turbulence around the microphones, which is typically correlated over small length scales. Source powers can then determined using conventional beamforming. The total source power from the model can then be determined using integration or a partial deconvolution technique such as CLEAN, which assists in the rejection of background noise[4].

In this paper we explore the differences between measurements from nested microphone arrays in the Markham wind tunnel at Cambridge University. Nested arrays are used to span a wider frequency range than is possible with a single array. Ideally, spectra from the two arrays will 'overlap' so that either array can be used in the centre of the spectrum. In practice, achieving a consistent spectral measurement from a test model can be difficult. At any given frequency, each array will have a different view angle of the source and a different ability to reject background interference.

In this paper, we present a series of measurements of sources using both nested arrays of Figure 1-1. We observe significant differences between the spectra from the two arrays and propose methods for recovering a consistent spectrum. Whilst the discussion which follows is applied directly to the nested arrays in the Markham wind tunnel, the discussion may be of interest to any tunnel with substantial background noise.

1.1 Aeroacoustic Experiments

The Markham tunnel has a working section of 1.8 x 1.2m, with maximum flow speed of 58m/s. Previous experiments have been successful at identifying the location of major acoustic sources on aerofoil slats and simplified landing gear models[6]. Details of experiments on landing gear models are shown in Figure 1-1, with sample source maps from the larger, low frequency array. Table 1.1 describes a typical test setup.

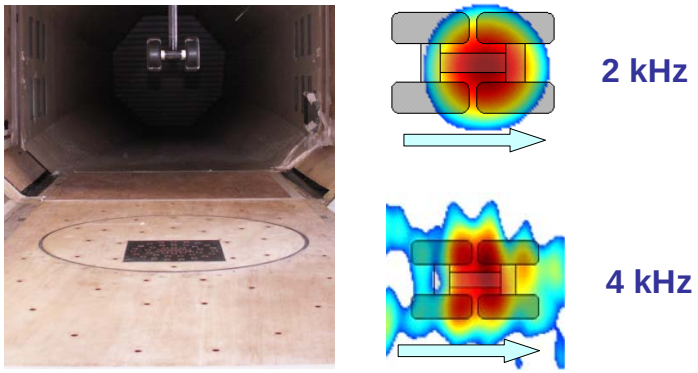

Figure 1-1-Markham Acoustic Arrays and typical landing gear noise measurements

	width (m)	length(m)	range	sample time	sample freq.
Low frequency (LF) array	1	1.8	1-5 kHz	600 s	30 kHz
High frequency (HF) array	0.3	0.3	5-30 kHz	180 s	120 kHz

Table 1.1-Array geometry and landing gear test data

1.2 Data processing

Data processing algorithms were implemented by P.Sijtsma of NLR[5, 7]. Auto-spectra are removed from the cross-power matrix before beamforming. In order to extract total source power, we prefer the CLEAN based on spatial source coherence (CLEAN-SC) method proposed by P.Sijtsma[7]. As with conventional CLEAN, this method identifies and successively removes peak sources from the source map along with sidelobes. CLEAN-SC also identifies sidelobes empirically using source cross-powers, rather than relying on mathematical point spread functions.

2 SPECTRA FROM A POWERED SOURCE

2.1 Simulated Monopole

We begin with a mathematically simulated monopole 0.6m above array centre, corresponding to a typical model location. The beamforming algorithm assumes a monopole source distribution and this simulation represents the 'ideal' measurement. Figure 2-1 shows source maps at 4kHz for both arrays and the integrated spectra obtained using CLEAN. Results are as expected, with the larger, low frequency array achieving better resolution for a given frequency but both arrays identifying the same source strength.

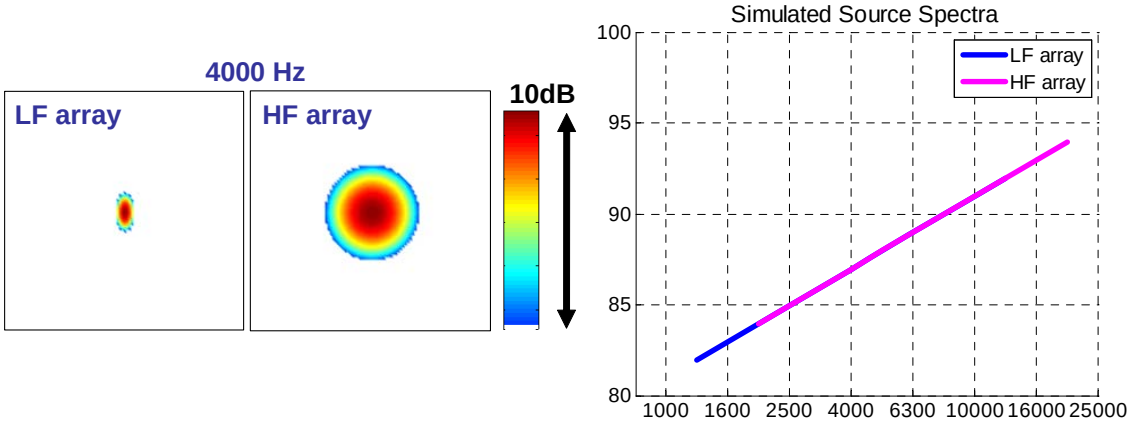

Figure 2-1-Source maps (4kHz) for both arrays using an ideal source; integrated spectra (CLEAN)

2.2 Experimental monopole

Whilst the theoretical monopole is easily constructed mathematically, a practical representation is more difficult to achieve. Verheij et al[8] obtained an approximation to the monopole using a horn driver connected with a narrow, rigid tube. With internal tube diameter 7mm, the source was monopole in nature at frequencies below 4kHz.

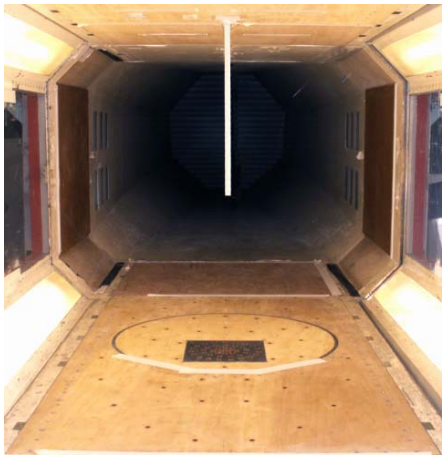

Figure 2-2-'Monopole' speaker source fitted in the Markham wind tunnel

In order to replicate the ideal source of Figure 2-1, we use a similar source with internal tube diameter 8mm (Figure 2-2). In the configuration shown, the source was found to have approximately uniform directivity over the area of the array for frequencies below 6kHz.

Figure 2-3 shows the spectra obtained by CLEAN with the source in the wind tunnel at constant amplitude. The source was examined with the wind tunnel off (0m/s) and at a speed of 30m/s. Above 6kHz, the non-uniform directivity of the source causes a drop-off in observed SPL from the low frequency array.

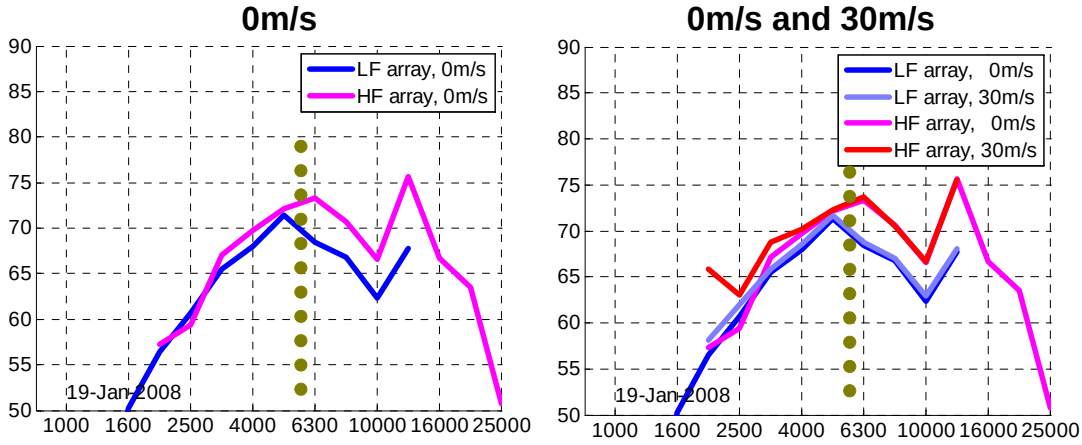

Figure 2-3-Monopole source in the Markham tunnel (a) 0m/s (b) 0m/s and 30m/s

Ideally, the low frequency (LF) and high frequency (HF) arrays would maintain their estimate of the source strength at 0m/s when the tunnel is turned on. In fact Figure 2-3(b) suggests that both arrays perform well in their design frequency range. Both arrays provide estimates within 1dB / third octave band for cases with and without flow.

3 AERODYNAMIC SOURCES OF SOUND

A series of landing gear models have been examined using the acoustic arrays[6]. In order to investigate noise sources around frequencies of interest, models were constructed at 1/12th

scale and examined at flow speeds of 50m/s. The Reynolds number was approximately $4x10^5$ (based on wheel diameter 0.1m). The model was placed in the centre of the tunnel, 0.6m above the arrays.

3.1 Experimental spectra

A 0.5m x 0.5m horizontal scanning plane was used for beamforming, with the centre of the plane at the centre of the model. CLEAN-SC was used to locate sources in the scanning plane, and any appearing at the model location were added to form the experimental spectrum. Figure 3-1 shows spectra for two landing gear configurations with different source mechanisms[6]. The spectra of Figure 3-1 are typical of measurements in other configurations. Experimental data were found to be repeatable to within 1dB / third octave band.

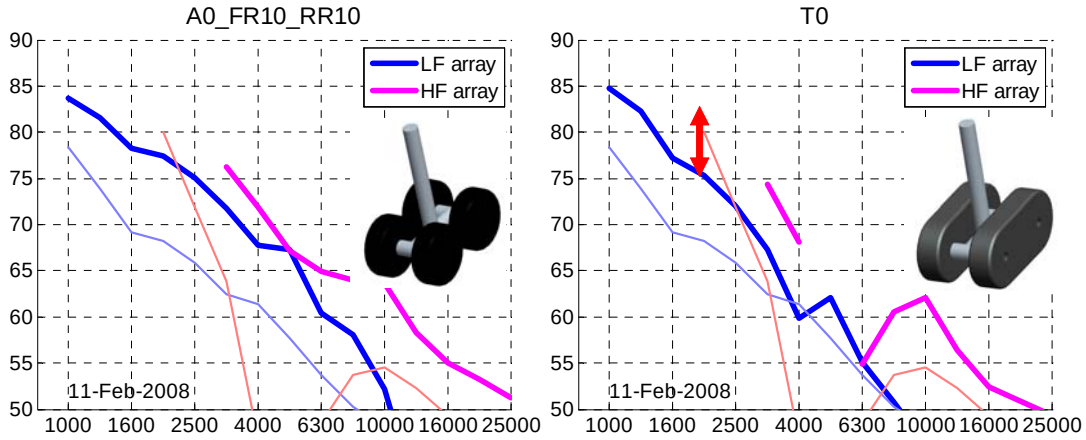

Figure 3-1-Landing gear spectra from the low(LF) and high (HF) frequency arrays

Model A0 is a generic, four-wheel landing gear with dressings, hoses and details removed. Model T0 is a similar model but with continuous 'tracks' fitted instead of wheels. These models have been used to help investigate the interaction between pairs of in-line wheels[6]. Figure 3-1 also shows empty tunnel spectra (dashed lines). Since no model was present, the empty tunnel levels are taken to be the maximum source power at any point in the scanning plane, rather than simply at the model location.

For both of the models in Figure 3-1, the arrays show differences in the noise spectra. At most frequencies, the HF array shows a higher noise estimate than the LF array for the same model. Some difference in noise level between the two arrays can be accounted for by directivity of the sources on the model. For the landing gear, the wheels shield some of the microphones at the edge of the LF array, reducing the noise estimate. The LF array can also be expected to underestimate source strength above 8kHz because of the large spacing between microphones.

At 4-6kHz the spectrum from the HF array appears to indicate lower noise levels than the surrounding spectra, particularly for model T0. Experiments with other landing gear and wing slat models have shown similar behaviour with the HF array at these frequencies[6]. The

effect is more severe when the model noise level is low, indicating the possibility of interference from another noise source in the tunnel. Source maps for the models of Figure 3-1 at 4kHz and 6kHz are shown in Figure 3-2. No background sources are seen in the area surrounding the model. However, the drop in measured noise away from the surrounding spectrum suggests that the model noise may be underestimated. This effect is not seen for data from the LF array.

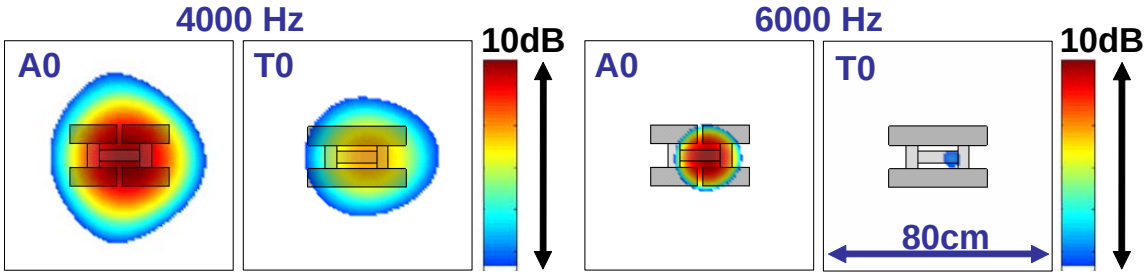

Figure 3-2-Source maps for the models of figure 2 at 4kHz and 6kHz (HF array)

3.2 Additional tunnel sources

In order to better understand additional sources in the wind tunnel, source maps were extended to an area of 1m x 1m around the model location for model T0 (Figure 3-3).

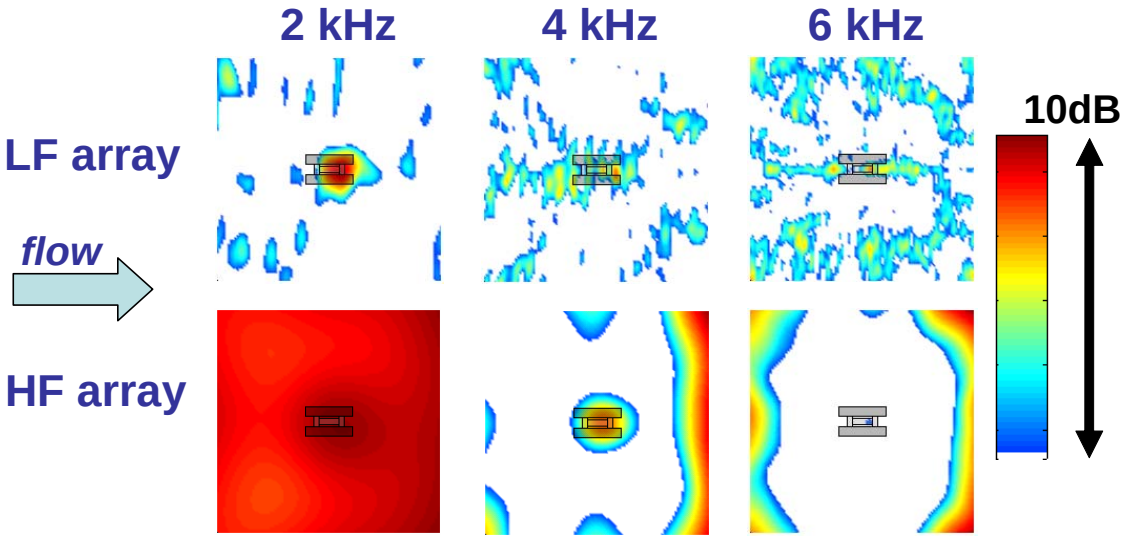

Figure 3-3-Extended source maps for model T0 (HF array)

Measurements from the HF array indicate a high amplitude source in the tunnel, which can also be seen without the model. The origin of this source is not clear. In addition to surface fittings in the working section, possible sources might include turning vanes, the fan, guide vanes or turbulence screen of the tunnel. Any source might also be reflected or transmitted around the hard wall tunnel so that the location cannot be clearly determined. However, this source was not removed by removing sharp details from the working section.

4 INFLUENCE OF AN UPSTREAM OR DOWNSTREAM SOURCE

4.1 A mechanism for interference

Figure 4-1 describes a simplified interference model. 'Source 1' is the acoustic source of interest (eg landing gear model) and 'Source 2' the upstream (or downstream) source. The sources are assumed to be incoherent but at the same frequency. We also begin by examining a two-microphone array with microphone spacing equal to one half of the wavelength for the frequency of interest, so that sound from source 2 is out of phase between the microphones.

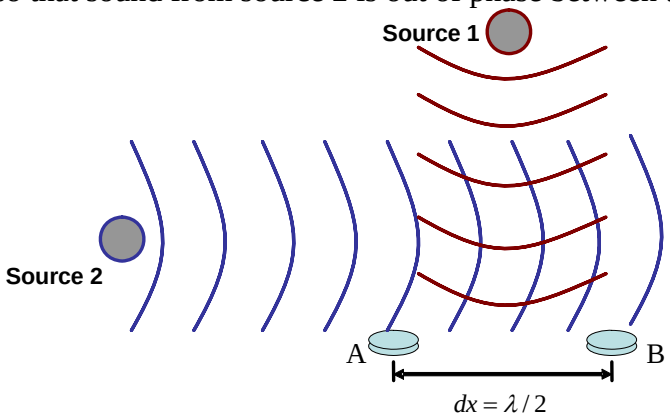

Figure 4-1-Two source, two microphone model of upstream interference

The following analysis uses the notation described by Sijtsma(CLEAN-SC/VKI). The amplitude of a unit source at distance r from each location can be described by:

$$g_1 = e^{-i\omega r_1/c} / 4\pi r_1 \qquad g_2 = e^{-i\omega r_2/c} / 4\pi r_2 \tag{1}$$

For the two-microphone array of Figure 4-1, the array steering vector for each source is given by the unit source strength at each microphone:

$$\underline{g}_1 = \frac{e^{-iwr_1/c}}{4\pi r_1}\begin{bmatrix}1\\1\end{bmatrix} \qquad \underline{g}_2 = \frac{e^{-iwr_2/c}}{4\pi r_2}\begin{bmatrix}1\\-1\end{bmatrix} \tag{2}$$

A cross spectral matrix, C, is then created using the cross-power between each pair of microphones in the acoustic array:

$$C_{AB} = \frac{1}{2} P_A P_B^* \qquad C = A_1 \underline{g}_1 \underline{g}_1^* + A_2 \underline{g}_2 \underline{g}_2^* \tag{3}$$

For the model of Figure 4-1, we consider sources which produce the same autopower levels at the microphones, producing a measured cross spectrum at the array as in equation 5.

$$C = A_1' \begin{bmatrix}1 & 1\\1 & 1\end{bmatrix} + A_2' \begin{bmatrix}1 & -1\\-1 & 1\end{bmatrix} \tag{5}$$

$$\frac{A_2}{A_1} = \frac{\left|g_1\right|^2}{\left|g_2\right|^2} \qquad A_2^{'} = A_1^{'} \tag{4}$$

In typical beamforming, we obtain an estimate of the source strength at location 1 using equation 6. The steering vector is known for each source location of interest and allows us to recover the true value of the original source:

$$A_1^{est} = \frac{\underline{g}_1^{*} C \underline{g}_1}{\left|g_1\right|^4} = \frac{A_1^{'}}{4} \begin{bmatrix} 1 & 1 \end{bmatrix} \begin{bmatrix} \mathbf{2} & 0 \\ 0 & \mathbf{2} \end{bmatrix} \begin{bmatrix} 1 \\ 1 \end{bmatrix} = \mathbf{A_1} \tag{6}$$

In a closed wind tunnel, however, microphone autopowers (diagonal cross power terms) are determined by the local boundary layer and cannot be used for beamforming. For beamforming in a closed test section, these are set to zero (equation 7). For the model in Figure 4-1, the result is an empty cross power matrix, with no information about the strength of source 1 because of the influence of source 2.

$$A_1^{est} = \frac{\underline{g}_1^{*} C \underline{g}_1}{\left|g_1\right|^4} = \frac{A_1^{'}}{4} \begin{bmatrix} 1 & 1 \end{bmatrix} \begin{bmatrix} \mathbf{0} & 0 \\ 0 & \mathbf{0} \end{bmatrix} \begin{bmatrix} 1 \\ 1 \end{bmatrix} = \mathbf{0} \tag{7}$$

Note that the matrix is empty because we assume the microphones to be one half wavelength apart. For any other spacing, the source estimate will not be zero, but it will be diminished. The equations above describe a simplified model of source interference for a two microphone array. The result is a ‘negative sidelobe’ of source 2, as described in experimental measurements by Sijtsma[7].

A practical array acoustic array has irregular microphone spacing and is more able to reject the interference described in Figure 4-1. For any array, the estimate of source 1 is provided by:

$$A_1^{est} = A_1 + \frac{\underline{g}_1^{*} C_2 \underline{g}_1}{\left|g_1\right|^4} = A_1 + A_2 \frac{\underline{g}_1^{*} \underline{g}_2 \underline{g}_2^{*} \underline{g}_1}{\left|g_1\right|^4} \tag{8}$$

Equation 8 suggests that the source estimate at location 1 might be reduced when beamforming without autopowers due to a source at location 2. Although a full array with irregular microphone spacing would not provide cancellation as suggested in Figure 4-1, a large amplitude A_2 can produce the same effect even when the product of steering vectors is only slightly less than zero. We simulate this effect in the following section.

4.2 Simulation of an downstream source

To examine the interference of an additional source in practice, two sources were set up in an anechoic chamber (Figure 4-2) using a loudspeaker and the source of Figure 2-2. Both sources were fed from separate signal generators and amplifiers to ensure incoherence. The loudspeaker produced broadband sound which was approximately 10dB louder than the overhead source at the microphone array location.

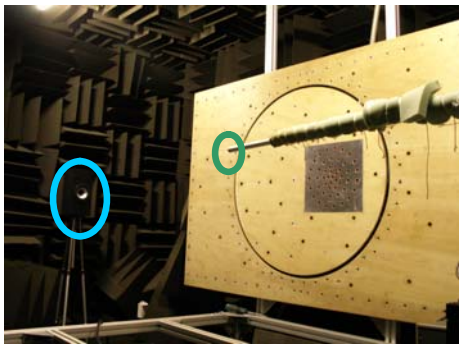

Figure 4-2-Experimental setup in an anechoic chamber

Figure 4-3 shows the effect of the 'downstream' source on the estimate of the 'overhead' source at 5kHz as well as a mathematical simulation of the interference using the same geometry. A clear reduction in estimated strength of the overhead source is seen when the downstream source is active.

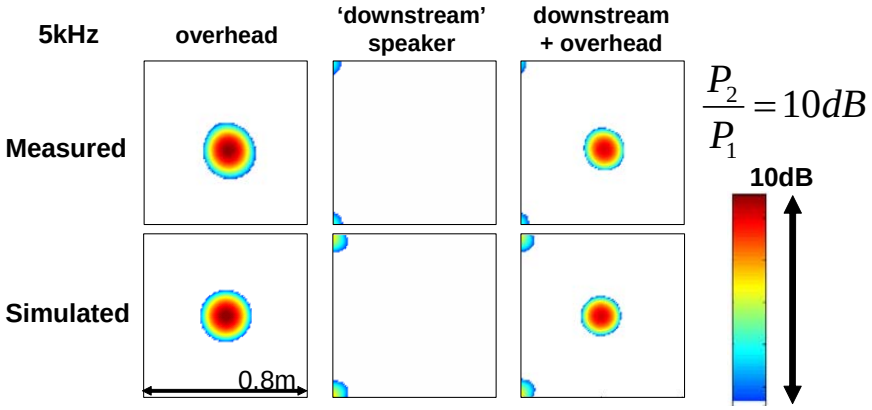

Figure 4-3-Simulated interference of an upstream source on the Markham HF array

Although this simulation is highly simplified, source maps can be seen to contain some of the features seen in the experiments of Figure 3-3. In particular, no sources are observed at the centre of the source map for the 'empty' configuration when only the upstream source is present. Measurements with both sources show a reduction in the overhead source estimate for both experiment and simulation.

5 REDUCING THE EFFECT OF UPSTREAM / DOWNSTREAM SOURCES

Whilst the effect of a single upstream source can be effectively simulated, it is difficult to extract the effect of such as source from tunnel measurements using beamforming. This is because source location and propagation through the tunnel are difficult to model. In this section, we consider using CLEAN-SC to extract a better estimate of model noise. This method is preferable to conventional CLEAN because it identifies coherent structures in the scanning plane, rather than relying on a theoretical beam pattern or 'point spread function'. A major advantage in the implementation of CLEAN-SC is that it provides restoration of these 'negative sidelobes' of the dominant downstream source in addition to the removal of 'positive' or regular sidelobes[7].

5.1 Capturing upstream / downstream sources

In order for CLEAN-SC to identify sources upstream or downstream, these need to be captured in the scanning grid. Whilst a grid which extends to the ends of the tunnel is quite impractical, a first step is to curve the ends of the scanning grid to the tunnel floor. A proposed scanning grid is shown in Figure 5-1.

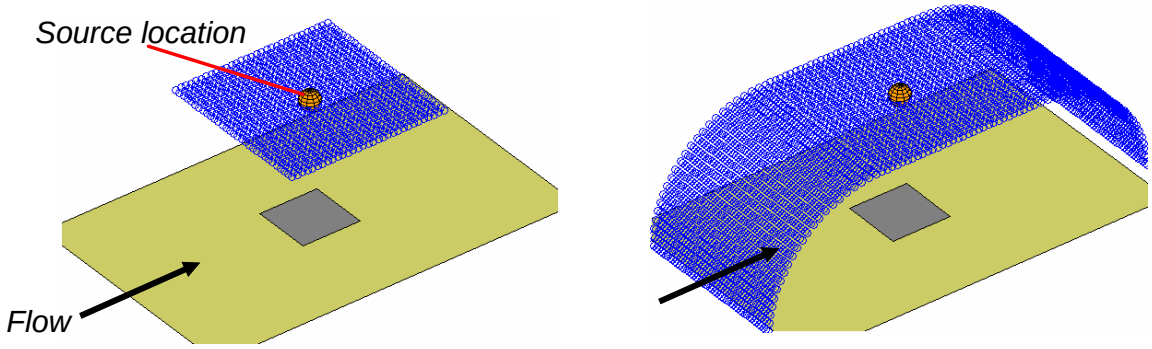

Figure 5-1-Scanning grids (a) typical (b) modified to capture upstream and downstream interference

Source maps using the new grid are shown in Figure 5-2. The HF array source map now clearly captures a strong source downstream of the model.

Figure 5-2-Beamforming source maps for model T0 using an adapted scanning grid (HF array)

When the beamforming result is analysed using CLEAN-SC, the algorithm identifies upstream and downstream sources in the first iterations because these sources have the highest amplitude. By 'cleaning' the source map, the effect of these sources on the model noise estimate is successively reduced.

5.2 Effect on experimental data

Figure 5-3 shows the effect of CLEAN-SC on measurements of the models in Figure 3-1 (only the centre of the source map is shown).

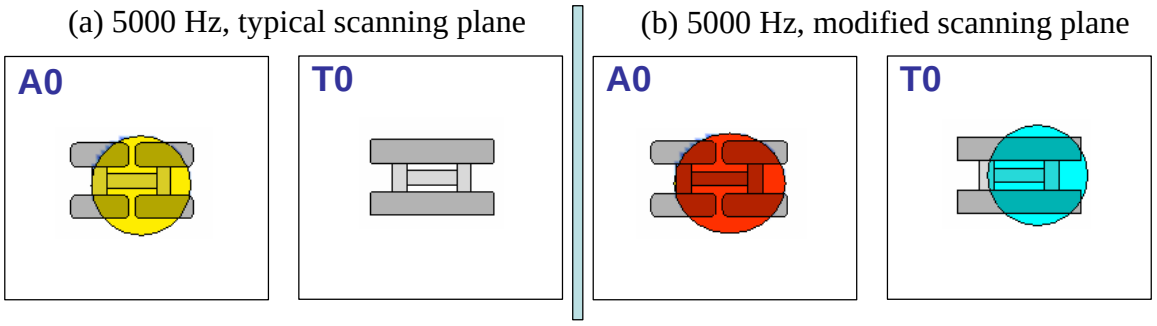

Figure 5-3-Models A0, T0 using CLEAN-SC for HF array data (a)tyipcal (b)modified grids (figure 5.1)

The effect of using the new scanning grid on source spectra is shown in Figure 5-4 for the models of Figure 3-2. At 4-6kHz, CLEAN appears to restore source powers for both models. Whilst the effect on the spectrum from model A0 is small, the array is now able to detect sources for model T0 that are in line with the rest of the spectrum (no sources were visible in the original source maps). There is also a clear reduction in the estimated noise level around 10kHz, though it is not clear whether this is a true reflection of noise generated by the model.

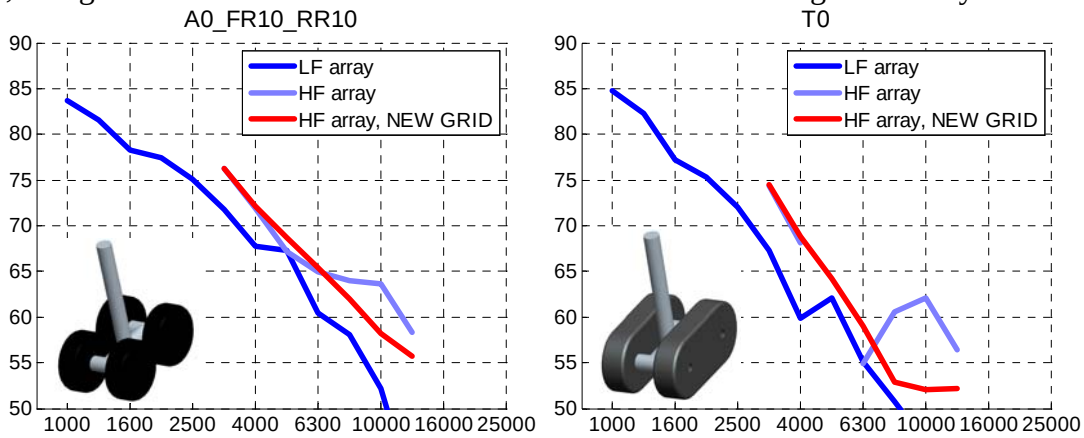

Figure 5-4-Spectra for model A0 with (a)typical and (b) modified scanning grids

5.3 Implications for experimental investigation

In the absence of accurate information about true source power, we present a series of measurements with models A0 and C2 in overhead and sideline directions[7]. Spectra are generated using the adapted scanning grid for HF array data.

Model A0 is a generic four-wheel gear containing only smooth wheels and axles. Measurements from Figure 5-5 suggest that sound generation at frequencies around 1-2kHz is directional. This is in line with the expectation that the axles generate dipole sound which has a directivity peak in the overhead direction[9]. At mid frequencies (2-5kHz) where wheel edges are known to generate noise[7], measurements suggest similar noise in both overhead and sideline directions. At the highest frequencies (above 6kHz), the closely spaced wheels appear to shield an observer at the sideline from much of the noise generated near the centre of the model.

Model C2 has differently shaped wheels which are widely spaced. The rounded front wheels promote flow instability and generate substantial scattering from the rear wheel leading edges[6], radiating noise in all directions. Noise levels are typically louder across the entire spectrum. Some directivity is seen at low frequencies, but sound produced at the wheel edges and from the main oleo / beam junction is now much more able to propagate to the microphones because of the widely spaced wheels. The result appears to be a spectrum which is consistent between arrays and between different model orientations.

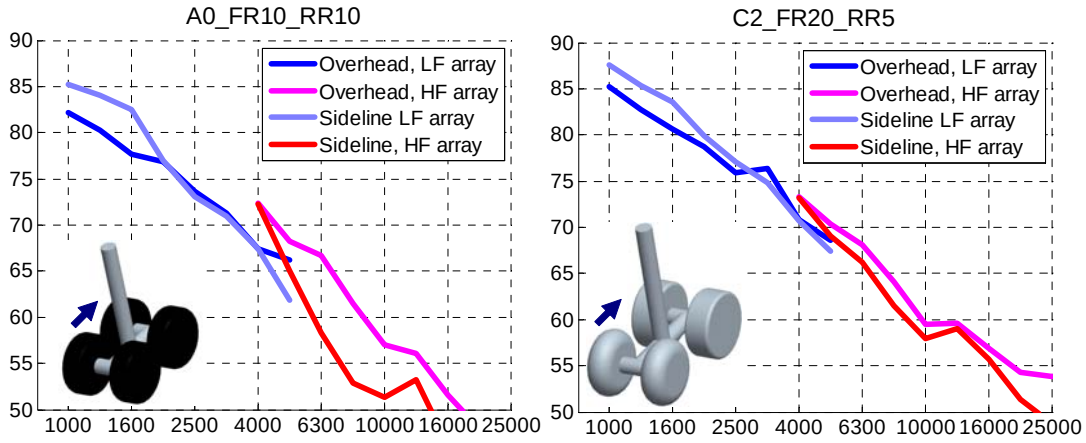

Figure 5-5-Overhead and sideline measurements of models A0 and C2

6 CONCLUSIONS

Obtaining spectra from closed wind tunnel measurements presents a range of challenges. The tunnel is a difficult environment for noise measurements and experiments have shown that subtle changes in model geometry can have a substantial effect on measured spectra, making it difficult to compare accurately with prior estimates of source strength.

It is well known that additional sources in a wind tunnel can amplify the estimate of sound obtained from a model. However, in most circumstances we can identify this interaction by examining sources visible in the model location with the tunnel empty.

In this paper we identify that sources in the tunnel may also substantially reduce noise estimates. This can occur even when there is little or no indication of background interference in source maps surrounding the model. We account for this negative interference effect in simulation and experiment.

Ideally, we would like to identify and remove additional sources from the tunnel. However, this may prove difficult and time consuming. Since CLEAN-SC allows empirical identification of coherent structures between points in the scanning plane, we were able to restore some of the original source strength by adapting the scanning grid to include sources at the ends of the tunnel. At present, it is difficult to evaluate the effectiveness of this (or a similar) technique without a series of detailed experiments using a known source strength. However, we were able to obtain consistent spectra between low and high frequency nested arrays for a range of low-noise landing gear configurations. As expected, spectra were more closely matched when the sources were more or less omni-directional.

REFERENCES

[1] W. M. Dobrzynski, L. C. Chow, P. Guion, and D. Shiells, "A European Study on Landing Gear Airframe Noise Sources," in *6th AIAA/CEAS Aeroacoustics Conference*: AIAA 2000-1971, 2000.

[2] R. W. Stoker and R. Sen, "An Experimental Investigation of Airframe Noise Using a Model Scale Boeing 777," in *39th AIAA Aerospace Sciences Meeting & Exhibit*. Reno, NV: AIAA Paper 2001-0987, 2001.

[3] Smith M.G., Fenech B., Chow L.C., Molin N., Dobrzynski W.M., and Seror C., "Control of Noise Sources on Aircraft Landing Gear Bogies," in *12th AIAA/CEAS Aeroacoustics Conference (27th AIAA Aeroacoustics Conference)*. Cambridge, MA: AIAA Paper 2006-2626, 2006.

[4] Quayle A.R., Dowling A. P., Babinsky H., Graham W.R., and Sijtsma P., "Landing Gear for a Silent Aircraft," in *AIAA Aerospace Sciences Meeting and Exhibit*. Reno, NV: AIAA Paper 2007-0231, 2007.

[5] Sijtsma P., "Experimental techniques for Identification and Characterisation of Noise Sources, in Advances in Aeroacoustics and Applications," VKI Lecture Series, 2004-05, 2004-05.

[6] Quayle A.R., Dowling A. P., Babinsky H., Graham W.R., and Y. Liu, "Mechanisms for Model Scale Landing Gear Noise Generation," in *AIAA Aerospace Sciences Meeting and Exhibit*. Reno, NV: AIAA Paper 2008-0016, 2008.

[7] Sijtsma P., "CLEAN Based on Spatial Source Coherence," in *13th AIAA/CEAS Aeroacoustics Conference (28th AIAA Aeroacoustics Conference)*. Rome, IT: AIAA Paper 2007-3436, 2007.

[8] J. W. Verheij, F. H. Van Tol, and L. J. M. Hopmans, "Monopole Airborne Sound Source With In Situ Measurement of its Volume Velocity," in *Internoise-95*. Newport Beach, CA, 1995.

[9] Lockard D.P., Khorrami M.R., Choudhari M.M., Hutcheson F.V., Brooks T.F., and Stead D.J., "Tandem Cylinder Noise Predictions," in *13th AIAA/CEAS Aeroacoustics Conference (28th AIAA Aeroacoustics Conference)*. Rome, IT: AIAA Paper 2007-3450, 2007.